

Quasicrystalline nature of quasicrystal surfaces: A photoemission study

D. Naumović, P. Aebi, and L. Schlapbach

Institut de Physique, Université de Fribourg, Pérolles, CH-1700 Fribourg, Switzerland

C. Beeli

Laboratory of Solid State Physics, ETHZ, CH-1015 Zürich, Switzerland

T. A. Lograsso and D. W. Delaney

Ames Laboratory, Iowa State University, Ames, Iowa 50011

Differently prepared surfaces of quasicrystalline *i*-Al-Pd-Mn are analyzed using angle-resolved photoemission in the x-ray and ultraviolet range of photon energies. Depending on the preparation, we find both surfaces with crystalline structure and metallic character, and surfaces with quasicrystalline structural fingerprints and a suppressed density of states at the Fermi level, compatible with a pseudogap.

Since their discovery, quasicrystals¹ have attracted much interest. It is the fascinating structure with five-, eight-, ten-, or 12-fold symmetry axes which brings up new challenges to conventional crystallography. Even today, the crystallographic structure is not entirely resolved. However, the electronic structure of quasicrystals is also peculiar. Quasicrystals exhibit an electrical resistivity thousands of times higher than that of their constituents.²

Specific heat measurements² indicated a significant reduction of the density of states (DOS) at the Fermi level E_F . Valence-band ultraviolet-photoemission spectroscopy (UPS) yielded conflicting results. Whereas Mori *et al.*³ reported a significant depression in the DOS at E_F for an *i*-Al-Cu-Fe alloy, a very high resolution study⁴ on a series of icosahedral alloys claimed the samples to be metallic, based on the observation of a clearly developed sharp Fermi edge. Both studies were done on scraped surfaces. On the other hand, angle-resolved UPS on a well-ordered monograin *i*-Al-Pd-Mn surface even showed some weak bandlike dispersion in the valence band, together with a distinct pseudogap feature at E_F .⁵ Very recently, an UPS and photon-energy-dependent core-level spectroscopy study on cleaved monograin *i*-Al-Pd-Mn demonstrated that the apparent metallicity at the surface is decreasing with increasing sampling depth.⁶

Together with the remarkable structural and electronic *bulk* properties we find unusually low wetting and friction on their *surfaces*. These are attributes that make quasicrystals also industrially attractive.⁷ On a fundamental level, it is, therefore, important to study differently prepared surfaces of a quasicrystal to see to what extent they are related to structural and electronic properties of the bulk. In particular, the geometrical and electronic structure has to be investigated in parallel.

Surface sensitive *structural* techniques have only been applied very recently.⁸⁻¹¹ Among them are scanning tunneling microscopy,⁸ secondary-electron imaging,⁹ low-energy electron diffraction (LEED),¹⁰ and x-ray photoelectron diffraction (XPD).¹¹ In structural surface studies it has been noticed

that different surface terminations are possible depending on the sample preparation: heat treatment, sputtering, or cleaving.⁸⁻¹²

It is, however, not clear what are the electronic structure fingerprints of such differently prepared surfaces. Therefore, we present a combined geometrical *and* electronic structure study on differently prepared *i*-Al-Pd-Mn monograin surfaces. The results clearly demonstrated that a sputtered surface that is appropriately annealed, shows all the structural fingerprints of a quasicrystalline structure together with distinct suppression of spectral weight in the DOS near E_F . In contrast, if the surface is disordered and the chemical composition is slightly changed, a crystalline surface structure is formed with a sharp metallic Fermi edge.

The photoemission experiments were performed in a VG ESCALAB Mk II spectrometer with a base pressure $\leq 5 \times 10^{-11}$ mbar. The sample stage is modified for motorized sequential angle-scanning data acquisition over a 2π solid angle.^{13,14} MgK $_{\alpha}$ radiation ($h\nu=1254$ eV) was used for x-ray photoelectron spectroscopy (XPS) in order to check the cleanliness of the sample and to determine the composition. UPS measurements were performed with monochromatized He I $_{\alpha}$ radiation (21.2 eV).¹⁵ The energy resolution of the analyzer for the UPS measurements was set to 30 meV. All measurements were performed at room temperature.

The *i*-Al-Pd-Mn quasicrystal ingot with its twofold axis parallel to the surface normal has been grown using the Bridgeman method (Ames Laboratory). Its stoichiometry was determined to be Al_{69.8}Pd_{20.0}Mn_{10.2}. It was oriented within 0.25° and polished with diamond paste and colloidal silica.¹⁶ The sample was a 1.3-mm-thick disk with a diameter of 15 mm. It was cleaned *in situ* by Ar⁺ sputtering at 1 and 0.75 kV (total time: 30 to 60 min) followed by annealing at indicated temperatures during 5 min (an additional 10 min were necessary to reach the desired temperature). Temperature was controlled with a pyrometer.

In the present study, the geometrical structure of the surfaces has been investigated by XPD.¹⁷ Briefly, in angle-scanned XPD x-ray photoemission peaks are measured as a function of emission angle and mapped stereographically in

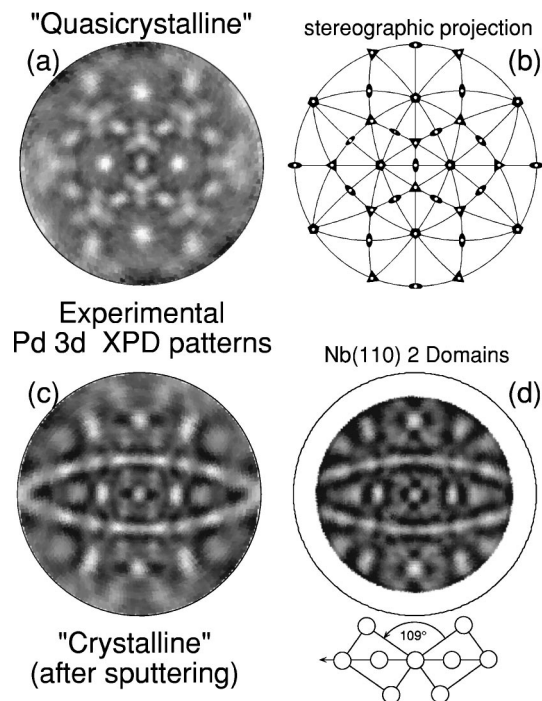


FIG. 1. (a) XPD pattern of a quasicrystalline surface of *i*-Al-Pd-Mn cut perpendicularly to a twofold symmetry axis obtained after standard preparation (sputtering and annealing at 650 °C) (Pd $3d_{5/2}$, $E_{\text{kin}} = 917$ eV). (b) Stereographic projection of the icosahedral symmetry elements, i.e., axes of two- (ellipses), three- (triangles) and fivefold (pentagons) symmetry. (c) A reconstruction of the surface appears after Ar^+ sputtering. (d) Superposition of two experimental XPD patterns from a Nb(110) single crystal (Nb $3d_{5/2}$, $E_{\text{kin}} = 1051$ eV) rotated by 109° with respect to each other as indicated.

a linear grayscale representation. High and low intensities are drawn in white and black, respectively. Normal emission corresponds to the center of the plot, whereas emission parallel to the surface, i.e., the 90° polar emission angle, is indicated by an outer circle (Fig. 1). XPD allows for a very simple interpretation in the case of photoelectron kinetic energies above approximately 500 eV.¹⁷ Photoelectrons leaving the emitter atom are strongly focused in forward direction by the neighboring atoms. The measured intensities are therefore high along densely packed atomic rows and crystallographic planes. Furthermore, in this energy regime, the so-called forward focusing is only weakly dependent on the atomic number Z . The position of the maxima thus basically depends only on the local geometrical structure, and the pattern represents a simple fingerprint of the crystallographic arrangement near the surface.

Figure 1(a) shows the angular distribution of the Pd $3d_{5/2}$ photoemission line intensity. The surface of the *i*-Al-Pd-Mn monograin cut perpendicularly to a twofold symmetry axis has been sputtered and annealed to 650 °C. Its XPS composition is found to be $\text{Al}_{73}\text{Pd}_{22}\text{Mn}_5$.¹⁸ Due to the forward-focusing properties of photoelectrons in the keV regime, the pattern nicely highlights densely packed high-symmetry (two-, three- and fivefold) axes of the icosahedral point group, as displayed in Fig. 1(b) (also in stereographic projection). The experiment can also be reproduced by single-scattering cluster calculation using clusters as inferred from structural mod-

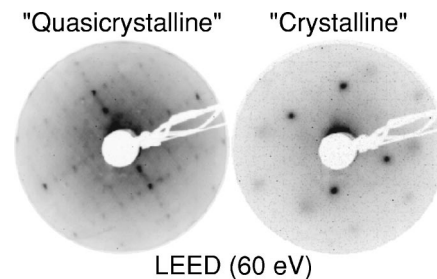


FIG. 2. LEED pattern of the “quasicrystalline” and the “crystalline” phase taken with electrons of 60 eV (high intensity in black).

els of the *i*-Al-Pd-Mn phase¹¹ giving a strong indication that the near surface region (within the escape depth of the photoelectrons) of this surface preparation is characteristic of a quasicrystalline structure. In strong contrast to Fig. 1(a), Fig. 1(c) displays the XPD pattern of a sputtered surface. This surface is disordered and exhibits a changed composition of $\text{Al}_{54}\text{Pd}_{42}\text{Mn}_4$. Locally, however, ordering persists, manifest as well-defined anisotropies in the XPD angular distribution of Fig. 1(c). This pattern can be understood by two domains of a cubic bcc(110)-like structure when comparing it with Fig. 1(d) where two measurements taken from a Nb(110) (bcc) single crystal, rotated by 109° , are superimposed. Therefore, the sputtered surface corresponds to two approximately equally populated domains of an Al-Pd alloy with a bcc lattice.

Annealing the sputtered surface first develops the cubic, crystalline structure up to ~ 400 °C and then becomes quasicrystalline. The corresponding LEED patterns are shown in Fig. 2. Note that even the sputtered surface shows diffuse LEED spots¹¹ which become sharper with annealing, and change into the “quasicrystalline” pattern (Fig. 2, left).

Figure 3 displays valence-band spectra taken at room temperature of the sputtered and annealed surfaces. We note two

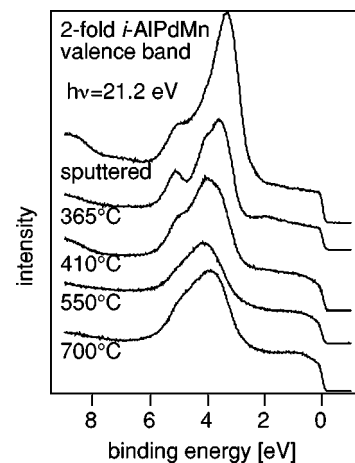


FIG. 3. Room-temperature valence-band spectra, taken with monochromatized He-I radiation ($h\nu = 21.2$ eV), of sputtered and annealed (as labeled) surfaces. Annealing corresponds to heating the sputtered surface (starting at room temperature) up to the labeled temperature. XPS concentrations for the different spectra are: $\text{Al}_{54}\text{Pd}_{42}\text{Mn}_4$ (sputtered surface), $\text{Al}_{61}\text{Pd}_{37}\text{Mn}_2$ (365 °C), $\text{Al}_{70}\text{Pd}_{26}\text{Mn}_4$ (410 °C), $\text{Al}_{73}\text{Pd}_{22}\text{Mn}_5$ (550 °C), $\text{Al}_{68}\text{Pd}_{27}\text{Mn}_5$ (700 °C).

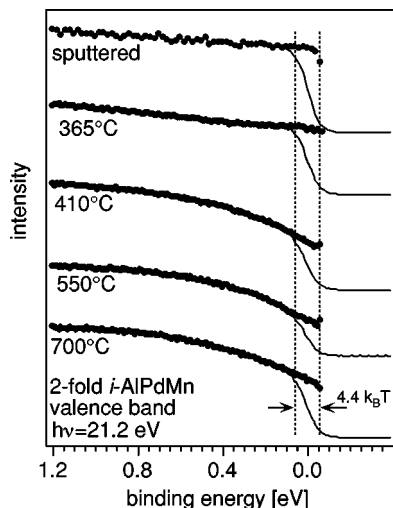


FIG. 4. Closeup of spectra of Fig. 3, displaying the near E_F region; spectra (thin black lines) are divided by the Fermi-Dirac distribution calculated for an effective (room) temperature obtained from the spectrum of the sputtered surface (see text); all spectra are taken at room temperature; labels indicate the annealing temperature.

important features developing with surface treatment: first, the characteristic change of the shape of the Fermi edge, which is shown in a close-up in Fig. 4; second, the shifting and splitting of the strongest peak at approximately 4-eV binding energy. Along with these systematic changes go structural fingerprints of the XPD and LEED experiments. Surfaces of the two topmost curves clearly show the crystalline patterns shown in Figs. 1 and 2, whereas surfaces of the three lowermost spectra display the quasicrystalline characteristic. LEED corresponding to the spectrum of the 410 °C annealed surface exhibits a higher background intensity, and the 365 °C annealed surface exhibits sharper spots than the respective quasicrystalline and crystalline pattern shown in Fig. 2. The prominent 4-eV feature (Fig. 3) has been attributed to Pd 4*d* electron states.¹⁹ A distinct shifting towards a higher binding energy is observed, reaching a maximum for the 550 °C surface. The shifting and splitting can be attributed to a specific chemical environment of near surface and surface Pd atoms. It is also interesting to note that qualitatively, the ratio of the 4-eV peak and the spectral weight close to E_F (attributed to Mn 3*d* states⁴) scales with the measured XPS composition: namely, high and low Pd concentration for the sputtered and “quasicrystalline” surface, respectively, and the highest Mn concentration for the “quasicrystalline” surface.

Figure 4 shows the same spectra (fine black lines) as in Fig. 3, zooming in closer to E_F . The black dots have been obtained by normalizing the spectra with the Fermi-Dirac distribution function,²⁰ therefore removing the sharp cutoff and creating a spectral function representing the DOS near E_F within a range of approximately $4.4 k_B T$, where k_B is the Boltzman constant.^{6,21} $4.4 k_B T$ represents the region where the Fermi-Dirac distribution function takes values between 90% and 10%. We clearly see that the two crystalline surfaces exhibit a linear behavior over the complete range of energies. For the 410 °C, 550 °C, and 700 °C surfaces, the shape is completely different. There is a distinct decrease of DOS towards E_F which can be interpreted as a pseudogap.

Different functions have been proposed to fit this decrease of DOS. Mori *et al.*³ used a linear function multiplied with a Lorentzian subtracted from unity. Then, the amplitude of the Lorentzian gives a measure for the depth of the pseudogap and its width indicates the width of the pseudogap. On the other hand, Wu *et al.*⁵ used an expression of the form $\propto (1 - E/E_F)^\alpha$ connecting to the square-root behavior of a Van Hove singularity. Tunneling spectroscopy²² and photoemission²³ data have also been fitted using a \sqrt{E} contribution in connection with a scaling theory of the metal-insulator transition in amorphous materials.²⁴ However, we find that a \sqrt{E} fit or even one of the form $a + b(E)^\alpha$ is very much dependent on the energy range used for the fit and only reasonable on a very small interval. Using the unity minus Lorentzian approach,³ nice agreement is obtained over an interval of more than an eV (not shown). The drawback of this procedure, however, is that parameters strongly depend on the slope of the linear function used to multiply, and this slope is arbitrary. It is, therefore, very difficult to give reliable numbers of size, width, and position of a pseudogap. Despite this difficulty, we note from the (Fermi-Dirac) normalized data in Fig. 4, that the DOS at E_F is reduced. The decrease of DOS extends over several hundred meV and the minimum in the DOS does not appear at E_F , rather is situated above, consistent with Neuhold *et al.*⁶

We can thus conclude that sufficiently high annealed surfaces exhibit *both* the structural *and* electronic fingerprints of a quasicrystalline surface, and one may call them quasicrystalline. However, although the structural probes (LEED for the long-range and XPD for the short-range order) are compatible with a quasicrystalline structure and there is a reduced DOS near E_F as predicted by many models, it is not clear whether quasicrystallinity is necessary to find this behavior. Similar experiments on approximants are needed to give a definite answer.

Furthermore, it is not clear if the depression of DOS is sufficient to explain the strongly reduced conductivity of quasicrystals or whether an unusually small electron diffusivity has to be considered.²⁵ Finally, one should mention another possibility where photoemission may mimic a pseudogap.²⁶ There, a sharp Fermi edge is destroyed through extrinsic, ohmic losses induced through the photoelectron, leaving a poorly conducting solid. Such an explanation is, however, in contradiction with the recent observation of a sharp Fermi edge in high resolution photoemission at low temperatures.⁴

In conclusion, a sputtered as well as a slightly (365 °C) annealed surface of a *i*-Al-Pd-Mn quasicrystal shows a crystalline and metallic behavior. In turn, if the sputtered surface is annealed to higher temperatures, (410 °C, 550 °C, 700 °C) the structural (LEED, XPD) and electronic characteristics (depression of spectral weight near E_F) show all the fingerprints expected for a quasicrystal. It is, however, not clear whether the quasiperiodicity is a necessary condition for this particular behavior or rather a complex atomic environment.

Skillful technical assistance was provided by E. Mooser, O. Raetz, R. Schmid, O. Zosso, Ch. Neururer, and F. Bourqui. This project has been supported by the Fonds National Suisse de la Recherche Scientifique.

- ¹D. Shechtman *et al.*, Phys. Rev. Lett. **53**, 1951 (1984).
- ²S.J. Poon, Adv. Phys. **41**, 303 (1992).
- ³M. Mori *et al.*, J. Phys.: Condens. Matter **3**, 767 (1991).
- ⁴Z.M. Stadnik *et al.*, Phys. Rev. Lett. **77**, 1777 (1996).
- ⁵X. Wu *et al.*, Phys. Rev. Lett. **75**, 4540 (1995).
- ⁶G. Neuhold *et al.*, Phys. Rev. B **58**, 734 (1998).
- ⁷J.-M. Dubois, Phys. Scr. **T49**, 17 (1993); *New Horizons in Quasicrystals, Research and Applications*, edited by A.I. Goldman *et al.* (World Scientific, Singapore, 1997); *Quasicrystals*, edited by J.-M. Dubois *et al.* (Materials Research Society, Pittsburgh, 1999).
- ⁸T.M. Schaub *et al.*, Phys. Rev. Lett. **73**, 1255 (1994).
- ⁹M. Erbudak *et al.*, Phys. Rev. Lett. **72**, 3037 (1994).
- ¹⁰T.M. Schaub *et al.*, Z. Phys. B **96**, 93 (1994).
- ¹¹D. Naumović *et al.*, Surf. Sci. **433-435**, 302 (1999); D. Naumović *et al.*, in *Proceedings of ICQ-6*, edited by S. Takeuchi, and T. Fujiwara (World Scientific, Singapore, 1998), p. 749; D. Naumović, *et al.*, in *New Horizons in Quasicrystals, Research and Applications* (Ref. 7), p. 86.
- ¹²Z. Shen *et al.*, Phys. Rev. Lett. **78**, 1050 (1997); Z. Shen *et al.*, Phys. Rev. B **58**, 9961 (1998); Ph. Ebert *et al.*, Phys. Rev. Lett. **77**, 3827 (1996); Ph. Ebert, F. Kluge, and K. Urban, Surf. Sci. **433-435**, 312 (1999); J. Ledieu *et al.*, *ibid.* **433-435**, 666 (1999); F. Schmithüsen *et al.*, *ibid.* (to be published).
- ¹³J. Osterwalder *et al.*, Phys. Rev. B **44**, 13 764 (1991).
- ¹⁴D. Naumović *et al.*, Phys. Rev. B **47**, 7462 (1993).
- ¹⁵Th. Pillo *et al.*, J. Electron Spectrosc. Relat. Phenom. **97**, 243 (1998).
- ¹⁶C.J. Jenks *et al.*, Appl. Surf. Sci. **103**, 485 (1996).
- ¹⁷For a review, see, e.g., C.S. Fadley, Surf. Sci. Rep. **19**, 231 (1993).
- ¹⁸Note that XPS concentrations cannot directly be compared with a true stoichiometry because they are only based on intensity ratios including core-level cross sections; see Ref. 11.
- ¹⁹G.W. Zhang *et al.*, Phys. Rev. B **50**, 6696 (1994).
- ²⁰The parameters have been obtained by fitting the spectrum of the sputtered surface to a Fermi-Dirac distribution function. This accounts for the room temperature and the instrumental broadening.
- ²¹T. Greber, T.J. Kreutz, and J. Osterwalder, Phys. Rev. Lett. **79**, 4465 (1997).
- ²²T. Klein *et al.*, Phys. Rev. Lett. **74**, 3656 (1995).
- ²³T. Schaub *et al.*, Phys. Rev. Lett. (to be published).
- ²⁴W.L. McMillan, Phys. Rev. B **24**, 2739 (1981).
- ²⁵Z.M. Stadnik *et al.*, Phys. Rev. B **55**, 10 938 (1997).
- ²⁶R. Joynt, Science **284**, 777 (1999).